Published in final edited form as:
*NMR Biomed*. 2014 January ; 27(1): . doi:10.1002/nbm.3002.

# Prostate Cancer Detection and Diagnosis: The Role of MR and its Comparison to other Diagnostic Modalities – A Radiologist's Perspective

**Tobias Penzkofer**[#,§] and **Clare M. Tempany-Afdhal**[#]

[#]Division of MRI &Surgical Planning Laboratory, Department of Radiology, Brigham and Women's Hospital, 75 Francis Street, 02115 Boston, USA

[§] Department of Diagnostic and Interventional Radiology, Aachen University Hospital, RWTH Aachen University, Pauwelsstr. 30, 52074 Aachen, Germany

## Abstract

It is now universally recognized that many prostate cancers are over-diagnosed and over-treated. The European Randomized Study of Screening for Prostate Cancer (ERSPC) from 2009 evidenced that, to save one man from death of prostate cancer, over 1,400 men had to be screened, and 48 had to undergo treatment. Detection of prostate cancer is traditionally based upon digital rectal examination (DRE) and measuring serum prostate specific antigen (PSA), followed by ultrasound guided biopsy. The primary role of imaging for the detection and diagnosis of prostate cancer has been transrectal ultrasound (TRUS) guidance during biopsy. MRI has traditionally been used primarily for staging disease in men with biopsy proven cancer. It is has a well-established role in detecting T3 disease, planning radiation therapy, especially 3D conformal or intensity modulated external beam radiation therapy (IMRT), and planning and guiding interstitial seed implant or brachytherapy. New advances have now established prostate MRI can accurately characterize focal lesions within the gland, an ability that has led to new opportunities for improved cancer detection and guidance for biopsy. There are two new approaches to prostate biopsy are under investigation both use pre-biopsy MRI to define potential targets for sampling and then the biopsy is performed either with direct real-time MR guidance (in-bore) or MR fusion/registration with TRUS images (out-of-bore). In-bore or out-of-bore MRI-guided prostate biopsies have the advantage of using the MR target definition for accurate localization and sampling of targets or suspicious lesions. The out-of-bore method uses combined MRI/TRUS with fusion software that provided target localization and increases the sampling accuracy for TRUS-guided biopsies by integrating prostate MRI information with TRUS. Newer parameters for each imaging modality such as sonoelastography or shear wave elastography (SWE), contrast enhanced US (CEUS) and MRI-elastography, show promise to further enrich data sets.

## Introduction

Prostate Cancer is a major public health issue that presents many challenges, it is the most frequent cancer in male patients in the developed world (1). Despite its very high incidence, however, only a small (2-4%) number of men will die from the disease. A desired but elusive goal is still the ability to prospectively identify the lethal cancers in a given population of men. Much effort is now devoted to this critical need, especially with increasing recognition of prostate cancer's over-diagnosis and over-treatment.

A current debate in medicine is focused on the merit of measuring the serum prostate specific antigen (PSA) for prostate cancer screening (2). The introduction of serum PSA testing, in the so-called “PSA era” led to a significant increase in the incidence of the disease

and has been blamed for contributing to the over-diagnosis situation; while a positive PSA test signals an increased risk for prostate cancer, its low specificity and the associated risk for unnecessary intervention such as biopsy and ultimately prostatectomies result in a classic screening dilemma. A new milestone was recently reached in 2012 with the assignment of a "d" grade to the test by the US Preventive Screening Task Force (USPSTF); it is now predicted that this will lead to the end of the "PSA era" (3,4). It remains to be seen if this will cause a reduction in overall diagnosis and morbidity. New strategies are called for to identify men with clinically significant disease who should have prostate biopsy and treatment.

Transrectal ultrasound (TRUS)-guided biopsies sampling 6-12 cores, 1-2 for each sextant, has been the diagnostic standard for prostate cancer for many years. This systematic approach has provided a simple, relatively easy, urology office-based test. The ultrasound images provide excellent guidance to the physician as to the gland size and boundaries but limited information regarding internal glandular tissue and little or no detail on focal lesions. The prostate tissue samples are obtained in a directed way via a needle aimed through the rectum to optimize the ability to sample the peripheral zone. Many areas, particularly the anterior gland, frequently are not sampled during TRUS biopsy. The method also has a possible risk of post-biopsy infection (rates 4-10%), and suffers from an inability to detect and diagnose clinically significant cancers (5-7).

Prostate MRI is now recognized as the most useful and accurate modality to detect, characterize and stage prostate cancer. Through combining different MRI-based techniques (T1-weighted [T1W], T2-weighted [T2W], diffusion-weighted imaging [DWI] and dynamic contrast enhanced imaging, [DCE]) it has become an increasingly utilized tool for prostate cancer diagnosis and staging. Now most centers performing prostate MRI use the multiparametric (mpMRI) approach (8,9).

Other biomarkers are under development and in testing for the clinical detection of prostate cancer, such as the urine test for PCA3 (10,11). Once we have a clear understanding of these technologies, assessment of their role relative to prostate MRI, may be warranted in order to provide clinically meaningful care for prostate cancer patients.

## MR-based detection of prostate cancer

The major advance in prostate MR has been the acceptance and now widespread practice of combining multiple MR parameters for an overall anatomical and functional assessment of the prostate gland tissues. The multiparametric prostate MRI (mpMRI) exam is generally performed as a combination of T1-weighted imaging, T2-weighted imaging, diffusion weighted imaging, and dynamic contrast enhanced imaging (Table 1) (12). Some centers will include MR spectroscopy (MRSI), which can be very useful in adding a metabolic assessment (13-15), though it is not currently listed as a requirement for prostate exams in a recent European consensus paper on prostate MRI methodology (16). MpMRI with either 1.5 or 3.0 Tesla magnets and with or without endorectal coil is now the preferred and recommended approach to all men presenting for prostate imaging. The use of an endorectal coil is optional and a subject of some debate (17,18). In recent years it has been shown that prostate MR imaging at 3T is feasible with sufficient image quality, even without using an endorectal coil (19,20). The recent European consensus does not list the use of endorectal as an essential requirement of MpMRI (16). However, endorectal coils do add to the available signal-to-noise ratio, which can be applied to gain higher spatial detail and contrast (21).

Despite its versatile capabilities, MRI is not as widely available or as easy to apply to prostate imaging, as ultrasound. Issues of cost, access, technical requirements and radiologists' acceptance and understanding of the procedure are continuing challenges. The

mpMRI exam can be complex to interpret and requires new skills for many radiologists that are not yet standardized (17). Educational efforts are available through a variety of societies, meetings, webinars etc. and there are regular courses on the subject at national and international radiological meetings to assist novice radiologists and technologists technically and interpretatively to learn and apply mpMRI in their clinical practices. Further attempts to standardize prostate MRI and MRI-targeted biopsy reporting have recently been published and aim to improve the quality of the reports, especially in collaboration with the referring disciplines (16,17,22). The ultimate goal of this classification is to allow meaningful discrimination between suspicious and/or high grade lesions, which need further workup with biopsy and those "benign-appearing" lesions which not need to be biopsied and can be observed with PSA monitoring.

## MRI protocol for prostate MR

The examination is performed as an outpatient procedure and will typically take 40-50 minutes. The endorectal coil is usually placed after a digital rectal examination (DRE) and application of xylocaine gel. Localizer imaging with a large field of view in three planes is recommended, which can also be used to confirm correct placement of the endorectal coil, if applicable. It will also provide the technologist with important landmarks for successful application of total coverage of the gland, as required. The geometry of the acquired sequences should be as similar as possible, with respect to angulation and slice thickness and location, in order to allow cross-sequence comparisons, which are particularly important for the T1W and T2W sequences, as these two sequences need to be compared side by side on the initial phase of interpretations to detect and localize any residual blood remaining after the prostate biopsy.

*T1W imaging* can be performed as fast spin echo (FSE/TSE) imaging or using 2D gradient-echo sequences (GRE). As the intraglandular T1 contrast is low, T1W imaging is used to diagnose intraprostatic bleeding, a common finding after prior biopsies. Hemorrhage appears hyperintense on T1W images and hypointense on T2W images, thus regions of hemorrhage need to be identified to exclude false positives in T2W imaging. Recent publications correctly point out the importance of reviewing the so-called "hemorrhage exclusion" or "halo sign", which is defined as a well-defined area of hypointensity within a region of hyperintensity on T1W images (23,24). It is speculated that this may be due to reduced bleeding in cancerous prostatic tissue from diminished citrate concentration in comparison to healthy prostatic tissue. Additionally, the T1W images are very useful in combination with other sequences for assessment of T3 disease; they allow for clear delineation of the prostate capsule and the region of the neurovascular bundles (NVB). All prostate MRI protocols should include a T1W nodal survey to the level of the kidneys to exclude regional lymph node involvement. Abnormal nodes are detected on the basis of size-enlarged nodes of 6-10 mm.

*T2W imaging* is almost exclusively performed as fast spin echo sequences, in three orthogonal orientations (axial, sagittal and coronal). The subglandular regions, such as the peripheral zone (PZ), the transitional zone (TZ) and the central zone (CZ), are usually well defined. Suspicious T2W lesions are hypointense regions, sometimes with a "erased charcoal or chalk-smear" appearance, depicting the ill-defined borders of such lesions (Figure 1, Figure 2). Importantly, extracapsular involvement of the NVB or the seminal vesicles can be assessed in T2W imaging, complementing the findings on T1W sequences (Figure 3, Figure 4). Post external beam radiation changes can lead to an overall reduction of T2 signal in the prostate, which needs to be taken into account when assessing post-radiation therapy recurrence in T2W-imaging (Figure 5).

*DWI* depicts the diffusivity of water molecules within the tissue that is decreased in the densely packed cellular structures of prostate carcinomas; it is the most recent addition to the prostate MRI sequence set and regarded by many as the most exciting and most essential sequence along with T2W. DWI is generally performed with echo-planar-imaging (EPI), which has important consequences for susceptibility artifacts. Especially when using endorectal coils, the susceptibility differences between the air filled balloon and prostatic tissue can lead to pronounced distortion artifacts, which some groups overcome by filling the balloon with barium sulfate or perfluorocarbon (25-27). This process is slightly more time-consuming than air inflation and, perhaps for that reason, not widely used (28). The type of diffusivity depicted in DWI can be controlled through the b-value of the sequence, effectively sensitizing the sequence to slower or faster moving water molecules. The current recommendations are that this sequence be obtained with at least two b-values, one low and one high (>800 sec/mm$^2$). At our institution DWI is acquired at b=500 and b=1400 sec/mm$^2$, to our experience the higher b-value depicts any suspicious areas in the PZ very consistently (29). Although less pronounced with higher b-values, any native DWI has some amount of T2 contrast component (T2-shine-through) that can be reduced through calculating quantitative apparent diffusion coefficient maps (ADC-maps) (12). While hyperintense areas in DWI (without T2-shine through) are suspicious for cancer, in ADC maps these regions are hypointense, reflecting the diminished diffusion capacity. Recent evidence points to a correlation between higher Gleason grade and lower diffusivity (low ADC) in prostate cancer (30). Such a finding may in the future allow non-invasive assessment of histologic cancer grade (13,31,32). In general, at this time, an ADC below $1 \times 10^{-3}$ mm$^2$/s is regarded as suspicious for cancer (13,31-33) (Figure 1, Figure 2, Figure 3, Figure 4, Figure 5, Figure 6).

*Dynamic contrast enhanced imaging* can be performed as 3D-spoiled-gradient-echo (3D-SPGR) sequences. Protocols imaging 3D-volumes every 6-8s for around 5 minutes with an intermediate FoV provide a reasonable compromise between spatial and temporal resolution. On a typical PACS workstation the enhancement can be detected by direct inspection, comparison with the pre-contrast images, cine mode display and calculation of a subtraction set of images. While assessing the raw DCE imaging can be challenging, several post-processing and quantitative analysis techniques have been employed in prostate DCE that allow for a more detailed assessment of focal lesions. Thereby often the shape of the contrast enhancement curve is evaluated. This can be accomplished by distinguishing between the three classic enhancement curves (type 1: steady enhancement, usually benign, type 2: plateau of signal intensity, suspicious of malignancy, type 3: washout of signal intensity, strong suspicion of malignancy) (17,34). The shape of these enhancement curves is also analyzed when deriving the so called “empirical” pharmacokinetic maps from raw DCE imaging, where semi-quantitative descriptors are calculated on a per voxel basis. Frequently used empirical measures are: time to contrast peak (time-to-peak, TTP), maximum slope of the contrast enhancement curve (maximum slope, MaxSlope), area under the contrast enhancement curve (area-under-the-curve, AUC). Prostate cancer is characterized by a short TTP, high MaxSlope and a high AUC-value on the respective parameter maps. In contrast to these measures, which, due to their semi-quantitative nature, are not easily comparable, quantitative measures have been developed. These parameters are calculated based on pharmacokinetic models, numerically assessing the contrast agent distribution in the tissue. Several of these models are used clinically with the Toft's model being one of the most common (35). Typical parameters calculated in pkMaps include $K^{trans}$, the forward volume transfer constant, expressing the amount of contrast agent transferred from between the blood plasma and the interstitial space and $v_e$, the fractional volume of interstitial space per volume. As a result of increased perfusion, $K^{trans}$ is elevated in prostate cancer, as a consequence of high cellular density, $v_e$ is reduced (Figure 1, Figure 2). The data acquisition is complex, and baseline pre-contrast imaging is critical once

validated T1 mapping methods have been assessed (36). Commercial software products are available that can process the raw DCE data and display the pharmacokinetic parameter maps and results on a workstation. When considering these products it is important to understand how the data is analyzed and displayed. One issue is the selection of threshold for color displays in terms of what cut points to use and how to validate them.

## Prostate Imaging Challenges

The typical patient populations presenting for prostate MRI are men either with confirmed or suspicion for prostate cancer. In the first group, the role of the exam is to stage the tumor for treatment planning, in case of patients on active surveillance (AS) to assess eligibility for or continuation in the AS protocol, or for patients who have already received treatment to monitor response to treatment. In the group of patients with no histologically confirmed prostate cancer, the goal is to detect and characterize all focal lesions for possible targeted biopsy. The focus in these patients is almost 100% on intra-glandular disease.

Prostate MR imaging of men without a prior cancer diagnosis is increasingly being used to define the presence or absence of intra-glandular suspicious lesions; it is an approach that is being promoted by a number of centers worldwide as a guide to biopsy (37-40) (Figure 7). Prospective trials should be used to determine if MR can be used to either replace the DRE and measurement of serum PSA approach or to supplement them prior to a biopsy. Diagnostic Prostate MRI and MRI guided biopsies are still in an early stage of scientific evidence. Most of the studies performed today evaluate end-points like cancer upgrading, detection rates of high-grade cancers in comparison to TRUS biopsies. Another aspect, which has not yet been evaluated long-term, is the potential for standardization of prostate MRI reports and classification of prostate MRI findings (16). Some early work has begun and more will follow. As always, attention should be paid to MR histological correlation, as the localization of suspicious prostatic lesions needs to be mapped against the imaging findings and due to the often multilocular and heterogeneous nature of the cancer mis-mapping of locations can be an issue. Different approaches have been developed to register histological localizations to radiological findings, common are: dividing the organ into reidentifiable sectors, cutting the prostate specimens consistent with image geometry, or radiology-histology computed co-registration (41-45). These methods offer good solutions and may be applied to avoid confounding correlations of tumor imaging with pathology results.

There are several imaging trials under way which will yield important information on the value of MR in detecting clinically significant disease: one prospective trial of template saturation core biopsy vs. mpMRI read prospectively will be important in determining the future of template based saturation biopsy approaches. The other important development will be the validation of ESUR PIRADS and the adoption by the international working group in collaboration with American College of Radiology (ACR).

## Prostate Image Guided Interventions and Intervention Planning

MR guided interventions are now performed at many centers worldwide (17,37,38,40,46). The technique is used for controlling and guiding thermal ablations in different diseases, ranging from cryoablation to MR guided focused ultrasound (47-49). At the Brigham and Women's Hospital, Boston (BWH) we pioneered several of these approaches to MR-guided prostate interventions (50). We established a MR-guided prostate brachytherapy program in 1997 and a transperineal MR guided biopsy (MRGB) program in 1999 (51-53). These two programs were performed using the open 0.5T Signa SP (GE healthcare, Milwaukee, USA). This open bore design allowed for easy access to the prostate via transperineal approach. Registration techniques from 3D-Slicer (www.slicer.org) were used to display pre-procedure

MR information combined with real-time gradient echo images and to control and guide the procedures. In 2010 we transitioned this program to 3.0T and use the wide bore (70cm) Siemens Verio device to continue our transperineal “in bore biopsy” MR guided program. The 3T wide bore magnet allows for relatively easy access to the prostate using a transperineal template approach. In the 15 years of the program, these procedures were successfully performed in over 1,000 men.

Using 3D Slicer we are able to perform on-line registration of pre biopsy data to intra-procedural image data. This enriches the information to the radiologist and with further rapid MR imaging we can track carefully the needle tip to the target. This was very helpful in guiding the placement of brachytherapy $I^{125}$ seeds, for implantation. The sub-total gland implantation was innovative approach and worked very well in low risk patients (54). One appealing aspect was the ability to implant any gland regardless of volume, without pubic arch interference. We continue to build on this experience with our on-going 3T biopsy program and in planning new focal therapy programs.

In general MRGB is either an “*in-bore*” or “*out of bore*” biopsy. The in bore approaches are exclusively MR based, using pre-biopsy MR to define the targets, real time MR to guide and control with image confirmation all steps of the procedure. The out of bore approaches use ultrasound to guide and control the procedure. The MR image-data is brought into the procedure either by image registration or “fusion” techniques or without them in the so-called “cognitive” biopsy. Clearly there are differences in technique and approach, but fundamentally the pre-procedure MR is critical for defining the target(s) and as described earlier this is should be done using mpMRI techniques. We will review the *in bore* approach and describe several of the *out of bore* approaches in the TRUS section below.

At BWH we are performing a prospective clinical trial of MRGB. All patients are selected based upon a clinical need - they have a rising PSA, prior negative TRUS biopsies, and suspicious lesion/targets on mpMRI, may have had prior treatment and suspected recurrence on mpMRI or are being evaluated for inclusion or continuation of active surveillance. A smaller group consists of men who have had prior rectal surgery which precluded TRUS access. This clinical research program is focused on several aims with an important one being the ability of mpMRI to detect significant cancers. This is a clinical research trial that involves pre-biopsy imaging as discussed above. All of the above mentioned diagnostic sequences (T2W, DWI, DCE, and PK-maps) are reviewed by three radiologists independently. Suspicious lesions are identified and marked. For each sequence and lesion, the confidence level is recorded along with each lesion on a 1-5 scale (1: definitely benign, 2: probably benign, 3: indeterminate, 4: probably malignant, 5: definitely malignant). Of all suspicious targets, a consolidated list of biopsy targets is compiled, and a biopsy plan created. During the biopsy, an intensity-based registration is performed to map the preprocedural MRI to the interventional coordinate system and to correct for prostate motion in cases of patient or organ movement as apparent on needle confirmations scans (55). A Z-Frame-based registration method is used to determine a template-based needle track using the open-source quantitative imaging platform 3D Slicer (www.slicer.org) (55-57) (Figure 7). Our results to date (58) have shown that this approach is very reliable, relatively easy and the targeted approach has high yield with more positive lesions coming from ADC and pharmacokinetic parameter positive sites.

## Transrectal Ultrasound (TRUS) and TRUS-guided biopsies

TRUS was introduced in the mid 1970's by Watanabe et al and has since been routinely used in pelvic imaging (59). Native TRUS allows for the depiction of the anatomy and volume of the prostate without in-depth insight into the prostate's fine structure (Figure 8). Sensitivity

and specificity for the detection of prostate cancer are poor (60-63). Another drawback is the high operator dependence of the ultrasound-based method in terms of interpretation and repeatability of the exam.

Many, but not all, prostate cancers manifest as hypoechoic lesions in native TRUS in the peripheral zone, but with as much as 40% isoechogenic PZ lesions, 5% hyperechogenic lesions and prostatitis and prostatic intraepithelial neoplasias also manifesting as hypoechogenic lesions. Therefore, the accuracy and sensitivity of TRUS for diagnosing prostate cancer are limited (60-63). The detection rates for TRUS as imaging modality are calculated to be around 11-35% (64,65). Hence, TRUS is not employed as a routine modality for targeted prostate biopsy but rather as guidance for systematic biopsies.

This is also reflected when using TRUS as a modality to guide prostate biopsies: Up to 30% of cancer missed when performing sextant biopsies (66), the method has been extended to 10-12 cores or as many as 45 cores for saturation biopsies with samples still being taken in a stochastic rather than a targeted manner (67). While taking more cores seems to improve the per patient detection rate of prostate cancer, the vastly invasive approach of placing up to 45 needles needs to be carefully taken into account.

## Problems with current TRUS prostate biopsy

Screening for prostate cancer is a controversial issue. Typical approaches have been to use a combination of DRE and PSA. Abnormalities in either test usually prompt a TRUS-guided prostate biopsy. The role of ultrasound in this setting is typically to guide the physician to the sites for biopsy by outlining the gland itself and allowing for systematic sampling by cognitive sub-division into sextant, octants or 12 symmetric locations. The advantages of this ultrasound-based technique are the relatively simple, user-friendly and inexpensive way the examination can be performed. The disadvantage is that this sampling approach is essentially “blind” to any local tissue characteristics. In contrast to all other image-based cancer diagnoses (such as breast biopsy), sampling in prostate cancer using ultrasound is not targeted.

## Elastography and enhanced Ultrasound techniques

Exploiting the mechanical properties, e.g. elevated stiffness resulting from higher cell and vessel density, of cancer tissue, ultrasound and MRI-based elastography are being used to assess the stiffness of tissue much like palpation and percussion of tissue. To take advantage of these distinctions for detection and diagnosis, ultrasound-based real-time elastography (called sonoelastography or RTE) is performed through manual compression of the tissue. A number of studies have been conducted for RTE. In a recent study with 139 patients, superior in per core cancer detection rates of targeted RTE biopsy over randomized ultrasound guided biopsy was shown (68), with the effect discernible in both patients undergoing repeat biopsy as well as patients with no previous biopsy. More than threefold of the cancers were detected by randomized biopsy compared to RTE only, suggesting an additional role of RTE-targeted biopsy rather than a replacement for the randomized approach. Another study evaluated RTE in a cohort of 109 patients with known prostate cancer before prostatectomy (69). In the whole-mount correlated setting, sensitivity and specificity values of 75.4% and 76.6% were established. While the study is certainly a hallmark for RTE-based prostate cancer diagnosis, the overall impact of the results remains unclear due to the selection bias for prostatectomy candidates. In another large cohort of 230 patients (70), a study showed superiority for RTE in malignant core percentage, even though a number of cancers were also detected by systematic biopsy and still other cancers were detected by systematic biopsies alone. The largest cohort to date was evaluated by Brock et al (71) who randomly assigned 353 patients with clinical suspicion for prostate cancer to

either grayscale TRUS-guided or RTE guided-biopsy, mainataing a 10-core systematic biopsy scheme. The RTE group had a significantly higher cancer detection rate (51.1% vs. 39.4%), although the authors state that the overall sensitivity remained low. MRI elastography relies on a defined mechanical excitation pattern applied through electronic actuators to determine tissue stiffness. In the case of prostate elastography this is achieved transurethrally(72), transrectally(73) or transperineally(74). However, all published studies are evaluating the technique at most centers in small sets of volunteers. So far, no clinical data is available for the technique (72-78).

Shear wave elastography is a further development of sonoelastography. Unlike the conventional approach where the operator needs to apply pressure to the tissue, here the ultrasound probe emits acoustic impulses that generate a defined shear wave that allows for quantitative evaluation of the tissue. Through this defined approach, SWE is deemed less operator dependent than previously mentioned forms of ultrasound. Early applications of this technique have been published in an ex-vivo setting, characterizing prostate cancer nodules (79), in an initial study in 53 patients for whom high sensitivity and specificity values were established (80). As in many of the new prostate imaging techniques, still larger patient cohorts need to be investigated.

The use of Doppler ultrasound has been studied by a number of groups as has, recently, the application of contrast-enhanced ultrasound for diagnosis of prostate cancer and the guidance of prostate biopsies (81,82). The rationale behind this approach is to employ imaging of tumor neovascularization as visualized by Doppler ultrasound for the detection of prostate cancer. Studies have shown an advantage of power Doppler ultrasound over color Doppler ultrasound (82), but still a wide range of diagnostic accuracy has been shown for Doppler ultrasound-based studies. Another potential application stems from studies showing a correlation between anomalies on Doppler ultrasound and higher Gleason grades of the tumors (83,84).

Histoscanning™ is an ultrasound-based technique, challenging the position of other cross-sectional prostate imaging modalities, especially prostate MRI (85,86). According to the information available, it applies a set of classification algorithms to the raw ultrasound radiofrequency data provided by a clinical ultrasound system. Based on these algorithms, regions suspicious for malignancies are marked on the ultrasound images to indicate the volume of the suspicious lesion. As there is only one vendor for the technique and a detailed description of the algorithms is not available, it remains a black box for much in-depth scientific evaluation. 3D reconstructions can be rendered within the system, promising easy visualization of the cancer burden and possibilities for nerve-sparing surgery. So far, a large patient cohort has not been studied. Published results concern between 14 and 80 patients (85-88); all studies have been conducted on subjects with known prostate cancer in advance of a radical prostatectomy. Currently five studies involving Histoscanning are listed on clinicaltrials.gov, four of which are actively recruiting (as of November 2012). From a radiologist's perspective Histoscanning™ is a tool for urologists. Radiologists are involved in any related prostate MRI work. However in light of the low evidence for the performance of Histoscanning, its clinical relevance remains unclear for the moment.

## MR-US-Fusion Systems

As in-bore interventions require MR scanners, thus valuable device time, they are associated with a higher organizational overhead due to the magnetic field hazards, MRI-guided prostate biopsy can be both time-consuming and expensive (38,89). It does however offer the only method which can image the target and the biopsy needle, within it, prior to sampling, thus the only true image targeted biopsy. A proposed solution for this dilemma is

the “out-of-bore” approach with fusion or registration of preprocedural prostate MRI imaging data to TRUS-guided biopsies that would combine the detection capabilities of MRI with the comparably easy setup of TRUS.

In a review by Moore et al (90) which analyzed reports on 16 distinct patient populations, this approach is not only deemed more accurate than untargeted (systematic) TRUS prostate biopsy, but also appears to reduce the diagnosis of insignificant cancer. At the same time, the targeted approach needs fewer total biopsies in the studies investigated.

The most straightforward approach for TRUS/MRI-guided biopsies is cognitive fusion where TRUS biopsies are performed knowing the localization of MRI-suspicious lesions derived from periprocedural MRI imaging. No specialized equipment is required other than a MRI scanner and a conventional TRUS biopsy device (89,90). Despite the fact that cognitive fusion seems to improve biopsy protocols, more sophisticated devices have been developed for MRI/TRUS fusion that use different ways of registering the intraprocedural ultrasound coordinates to the MRI coordinates. The two most frequently used methods are real-time MRI/ultrasound registration or electromagnetically tracked ultrasound probes that relate the two coordinate systems after an initial registration step. Singh et al (91) showed in a pilot study the feasibility and accuracy of MRI/TRUS-guided biopsies based on electromagnetic navigation and superimposed MRI/TRUS images. From the same group a more recent report was published applying MRI/TRUS electromagnetically guided prostate biopsy in a cohort of 195 men with previous negative biopsies. The system was directly compared to 12-core TRUS biopsy and MRI/TRUS fusion was able to identify more high grade cancers (21 vs. 11 men) and led to upgrading in a number of cases compared to US guidance (92)

Currently, a number of commercial MRI/TRUS fusion devices are available, including: Urostation, Koelis Promap MR and Promap 2L (Koelis, Grenoble, France), the Eigen Artemis ProFuse Bx system (Artemis; Eigen, Grass Valley, CA, USA), BiopSee™ (MedCom, Darmstadt, Germany), Hitachi RVS (Hitachi, Japan) (93), Invivo Uronav (Philips Medical, Best, The Netherlands), and the BioJet System (GeoScan, Lakewood Ranch, FL, USA).

Pinto et al studied a group of 101 patients of three different risk categories derived from imaging aspects (low, moderate, high) on a EMT/TRUS/MRI system developed with Philips (94). The system allowed for free hand manipulation of the TRUS probe and applied electromagnetic navigation to localize the current US imaging field-of-view within the MR dataset. All patients received 12-core standard systematic and MRI/TRUS fused prostate biopsies in the same setting. Cancer was detected in 27.9%, 66.7%, and 89.5% of the cases for the low, intermediate and high risk group, respectively. In this setting MRI/TRUS fusion-guided prostate biopsies detected more cancer per core than the standard 12 core approach (20.6% vs. 11.7%). Although this result is encouraging, and might lead to a lower number of biopsies performed with fused systems, on a per patient basis, of 55 patients in which prostate cancer was detected, 35 patients received a diagnosis from both systems, with 10 from TRUS alone and 10 from the MRI/TRUS combination.

The Artemis Eigen Device has been studied by Sonn et al in a group of 171 patients (6). While on a per core basis the authors concluded that TRUS/MRI biopsy is three times as likely to yield cancer diagnoses (21% of performed targeted biopsies vs. 7% of systematic biopsies), on a per patient basis, many cancers were detected by systematic biopsy alone (84 total positive diagnoses, 38 by both methods, 15 by MRI/TRUS alone, 31 by systematic TRUS-guided biopsy alone). Thus, the combination of systematic with TRUS-guided biopsy

seems to be key in detecting more cancers. As it can be performed in an office setting, the authors concluded that this method allows for a more efficient prostate cancer diagnosis.

The Urostation system was studied by Ukimura et al in a phantom setting (95), establishing a target error of 2-3 mm for different types of lesions. So far no patient study is published using this system.

A study performed by Kuru et al, using the commercially available BiopSee™ system in 50 consecutive patients, had a cancer detection rate of 54% (27 patients). The patients were further divided into subgroups and analyzed. In patients with highly suspicious lesions on prostate MRI in 100% of the cases a histological confirmation was achieved, whereas in patients with no prior prostate biopsy, the detection rate was 68%. As with many other studies a high per-core rate of positive biopsy results was achieved (53%). The authors compared these results with systematic TRUS-guided biopsies performed at the same session when only 7% of the cores were positive. These systematic biopsies had, however, been performed in areas of the prostate which appeared normal on prostatic MRI, potentially biasing this comparison. Further extending this study, results were published by Hadaschik et al (96) for a group of 106 patients with a detection rate of 59.4% overall and 95.8% in patients with high clinical suspicion for prostate cancer, confirming the results of the prior study.

While the Biojet system from GeoScan received FDA and EU CE approval in 2012, as of November 2012, no published clinical experience is available.

In all abovementioned approaches, MRI/MRI and TRUS/MRI fusion, accurate registration of imaging from different time-points is crucial for successfully performing procedures (51,55,56,97-100). Deformation and substantial mobility of the organ need a spatial correction to match preprocedural to intraprocedural imaging. Motion correction can be especially complicated when endorectal coils are used pre-procedurally but not during the procedure (21,55,101). Most of the various techniques developed are using non-rigid registration to correct biopsy target locations (55,102).

## CT and PET/CT

Computed tomography has a role in staging advanced prostate cancer, especially bone metastases, and pelvic lymph node spread. Although it is a major workhorse for nearly all malignancies, it has its limitations when it comes to prostate cancer imaging (66); despite many advances that have been made with respect to CT resolution, speed and contrast-enhanced CT scanning protocols, including CT perfusion, no clinical role has been identified in the detection primary prostate due to insufficient spatial and contrast resolution for the prostate (103,104). Similarly PET/CT is used for detecting prostate cancer spread or local/distant recurrence after treatment (similarly to prostate MRI, Figure 6), but so far no sufficient detection capability has been identified for primary prostate cancer diagnosis. $^{18}$F-Flurodesoxyglucose (FDG) was the first radiotracer studied, although limited sensitivity for challenged by PET-negative primary and metastatic prostate cancer lesions for $^{18}$F-FDG, the search for more suitable tracers began (105,106). Other tracers have been developed specifically for utilization in prostate cancer, such as 18-fluorodihydrotestosterone ($^{18}$F-FDHT), $^{11}$C-acetate, $^{11}$C-methionine, and choline derivates such as $^{11}$C-choline or $^{18}$F-choline. With the latter two being the most promising candidates, larger clinical trials assessing the benefit of PET/CT based therapy decisions or the comparison to MRI based techniques such as DWI and DCE are still awaited (105).

## Conclusion

Multi-parametric MRI with T2W, Diffusion (DWI) and dynamic contrast enhanced (DCE) sequences is now the established approach to prostate MRI. This technique allows for improved detection, characterization and staging of focal prostate cancer. Transrectal ultrasound guided biopsy is still the most frequently used guidance modality for diagnosing prostate cancer, although the procedure is performed in a systematic way, without direct visualization of suspicious lesions. On the other hand, MRI is currently the most widespread technique to detect prostate cancer noninvasively and is being increasingly used to guide targeted prostate biopsies. Several new approaches to directly visualize prostate cancer with ultrasound using elastography or sophisticated post-processing or using the information from prostate MRI during ultrasound employing fusion technologies, are currently under development in order to improve prostate cancer biopsy accuracy and yield.

## Acknowledgments

This work is supported by R01CA111288, P41RR019703, P01CA067165, U01CA151261, and U54EB005149 from NIH. Its contents are solely the responsibility of the authors and do not necessarily represent the official views of the NIH.TP receives funding from RWTH Aachen University Hospital.

## References

1. National Institutes of Health. Prostate Cancer. 2012
2. Carter HB, Albertsen PC, Barry MJ, Etzioni R, Freedland SJ, Greene KL, Holmberg L, Kantoff P, Konety BR, Murad MH, Penson DF, Zietman AL. Early Detection of Prostate Cancer: AUA Guideline. The Journal of urology. 2013
3. USPSTF. Screening for Prostate Cancer. 2012; 2012
4. Moyer VA. Screening for prostate cancer: U.S. Preventive Services Task Force recommendation statement. Annals of internal medicine. 2012; 157(2):120–134. [PubMed: 22801674]
5. Nam RK, Saskin R, Lee Y, Liu Y, Law C, Klotz LH, Loblaw DA, Trachtenberg J, Stanimirovic A, Simor AE, Seth A, Urbach DR, Narod SA. Increasing hospital admission rates for urological complications after transrectal ultrasound guided prostate biopsy. The Journal of urology. 2013; 189(1 Suppl):S12–18. [PubMed: 23234616]
6. Sonn GA, Natarajan S, Margolis DJA, MacAiran M, Lieu P, Huang J, Dorey FJ, Marks LS. Targeted Biopsy in the Detection of Prostate Cancer Using an Office Based Magnetic Resonance Ultrasound Fusion Device. The Journal of urology. 2012
7. Isariyawongse BK, Sun L, Banez LL, Robertson C, Polascik TJ, Maloney K, Donatucci C, Albala D, Mouraviev V, Madden JF, Moul JW. Significant discrepancies between diagnostic and pathologic Gleason sums in prostate cancer: the predictive role of age and prostate-specific antigen. Urology. 2008; 72(4):882–886. [PubMed: 18384857]
8. Yakar D, Debats OA, Bomers JG, Schouten MG, Vos PC, van Lin E, Futterer JJ, Barentsz JO. Predictive value of MRI in the localization, staging, volume estimation, assessment of aggressiveness, and guidance of radiotherapy and biopsies in prostate cancer. Journal of magnetic resonance imaging : JMRI. 2012; 35(1):20–31. [PubMed: 22174000]
9. Turkbey B, Choyke PL. Multiparametric MRI and prostate cancer diagnosis and risk stratification. Current opinion in urology. 2012; 22(4):310–315. [PubMed: 22617060]
10. Nakanishi H, Groskopf J, Fritsche HA, Bhadkamkar V, Blase A, Kumar SV, Davis JW, Troncoso P, Rittenhouse H, Babaian RJ. PCA3 molecular urine assay correlates with prostate cancer tumor volume: implication in selecting candidates for active surveillance. The Journal of urology. 2008; 179(5):1804–1809. discussion 1809-1810. [PubMed: 18353398]
11. Marks LS, Fradet Y, Deras IL, Blase A, Mathis J, Aubin SM, Cancio AT, Desaulniers M, Ellis WJ, Rittenhouse H, Groskopf J. PCA3 molecular urine assay for prostate cancer in men undergoing repeat biopsy. Urology. 2007; 69(3):532–535. [PubMed: 17382159]

12. Hegde JV, Mulkern RV, Panych LP, Fennessy FM, Fedorov A, Maier SE, Tempany CM. Multiparametric MRI of prostate cancer: An update on state-of-the-art techniques and their performance in detecting and localizing prostate cancer. Journal of magnetic resonance imaging : JMRI. 2013; 37(5):1035–1054. [PubMed: 23606141]
13. Kobus T, Vos PC, Hambrock T, De Rooij M, Hulsbergen-Van de Kaa CA, Barentsz JO, Heerschap A, Scheenen TW. Prostate Cancer Aggressiveness: In Vivo Assessment of MR Spectroscopy and Diffusion-weighted Imaging at 3 T. Radiology. 2012
14. Sciarra A, Panebianco V, Salciccia S, Gentilucci A, Alfarone A, Dimare L, Lisi D, Catturino S, Di Pierro G, Von Heland M, Ciccariello M, Passariello R, Gentile V. Value of magnetic resonance spectroscopy (MSR) and dynamic contrast-enhanced magnetic resonance (DCEMR) imaging for the characterization of high-grade prostatic intraepithelial neoplasia (HGPIN) foci. Urologic oncology. 2011; 29(6):634–640. [PubMed: 19914107]
15. Scheenen TW, Futterer J, Weiland E, van Hecke P, Lemort M, Zechmann C, Schlemmer HP, Broome D, Villeirs G, Lu J, Barentsz J, Roell S, Heerschap A. Discriminating cancer from noncancer tissue in the prostate by 3-dimensional proton magnetic resonance spectroscopic imaging: a prospective multicenter validation study. Investigative radiology. 2011; 46(1):25–33. [PubMed: 21188832]
16. Dickinson L, Ahmed HU, Allen C, Barentsz JO, Carey B, Futterer JJ, Heijmink SW, Hoskin PJ, Kirkham A, Padhani AR, Persad R, Puech P, Punwani S, Sohaib AS, Tombal B, Villers A, van der Meulen J, Emberton M. Magnetic resonance imaging for the detection, localisation, and characterisation of prostate cancer: recommendations from a European consensus meeting. European urology. 2011; 59(4):477–494. [PubMed: 21195536]
17. van de Ven WJ, Hulsbergen-van de Kaa CA, Hambrock T, Barentsz JO, Huisman HJ. Simulated required accuracy of image registration tools for targeting high-grade cancer components with prostate biopsies. European radiology. 2012
18. Eberhardt SC, Carter S, Casalino DD, Merrick G, Frank SJ, Gottschalk AR, Leyendecker JR, Nguyen PL, Oto A, Porter C, Remer EM, Rosenthal SA. ACR Appropriateness Criteria prostate cancer--pretreatment detection, staging, and surveillance. Journal of the American College of Radiology : JACR. 2013; 10(2):83–92. [PubMed: 23374687]
19. Kobus T, Hambrock T, Hulsbergen-van de Kaa CA, Wright AJ, Barentsz JO, Heerschap A, Scheenen TW. In vivo assessment of prostate cancer aggressiveness using magnetic resonance spectroscopic imaging at 3 T with an endorectal coil. European urology. 2011; 60(5):1074–1080. [PubMed: 21419565]
20. Scheenen TW, Heijmink SW, Roell SA, Hulsbergen-Van de Kaa CA, Knipscheer BC, Witjes JA, Barentsz JO, Heerschap A. Three-dimensional proton MR spectroscopy of human prostate at 3 T without endorectal coil: feasibility. Radiology. 2007; 245(2):507–516. [PubMed: 17848681]
21. Heijmink SW, Futterer JJ, Hambrock T, Takahashi S, Scheenen TW, Huisman HJ, Hulsbergen-Van de Kaa CA, Knipscheer BC, Kiemeney LA, Witjes JA, Barentsz JO. Prostate cancer: body-array versus endorectal coil MR imaging at 3 T--comparison of image quality, localization, and staging performance. Radiology. 2007; 244(1):184–195. [PubMed: 17495178]
22. Moore CM, Kasivisvanathan V, Eggener S, Emberton M, Futterer JJ, Gill IS, Grubb Iii RL, Hadaschik B, Klotz L, Margolis DJ, Marks LS, Melamed J, Oto A, Palmer SL, Pinto P, Puech P, Punwani S, Rosenkrantz AB, Schoots IG, Simon R, Taneja SS, Turkbey B, Ukimura O, van der Meulen J, Villers A, Watanabe Y. on behalf of the SC. Standards of Reporting for MRI-targeted Biopsy Studies (START) of the Prostate: Recommendations from an International Working Group. European urology. 2013
23. Barrett T, Vargas HA, Akin O, Goldman DA, Hricak H. Value of the hemorrhage exclusion sign on T1-weighted prostate MR images for the detection of prostate cancer. Radiology. 2012; 263(3): 751–757. [PubMed: 22474673]
24. Purysko AS, Herts BR. Prostate MRI: The Hemorrhage Exclusion Sign. The Journal of urology. 2012; 188(5):1946–1947. [PubMed: 22999551]
25. Prando A, Kurhanewicz J, Borges AP, Oliveira EM Jr. Figueiredo E. Prostatic biopsy directed with endorectal MR spectroscopic imaging findings in patients with elevated prostate specific antigen levels and prior negative biopsy findings: early experience. Radiology. 2005; 236(3):903–910. [PubMed: 16118169]

26. Turkbey B, Pinto PA, Mani H, Bernardo M, Pang Y, McKinney YL, Khurana K, Ravizzini GC, Albert PS, Merino MJ, Choyke PL. Prostate cancer: value of multiparametric MR imaging at 3 T for detection--histopathologic correlation. Radiology. 2010; 255(1):89–99. [PubMed: 20308447]
27. Rosen Y, Bloch BN, Lenkinski RE, Greenman RL, Marquis RP, Rofsky NM. 3T MR of the prostate: reducing susceptibility gradients by inflating the endorectal coil with a barium sulfate suspension. Magnetic resonance in medicine : official journal of the Society of Magnetic Resonance in Medicine / Society of Magnetic Resonance in Medicine. 2007; 57(5):898–904. [PubMed: 17457870]
28. Noworolski SM, Crane JC, Vigneron DB, Kurhanewicz J. A clinical comparison of rigid and inflatable endorectal-coil probes for MRI and 3D MR spectroscopic imaging (MRSI) of the prostate. Journal of magnetic resonance imaging : JMRI. 2008; 27(5):1077–1082. [PubMed: 18407539]
29. Kitajima K, Takahashi S, Ueno Y, Yoshikawa T, Ohno Y, Obara M, Miyake H, Fujisawa M, Sugimura K. Clinical utility of apparent diffusion coefficient values obtained using high b-value when diagnosing prostate cancer using 3 tesla MRI: comparison between ultra-high b-value (2000 s/mm(2)) and standard high b-value (1000 s/mm(2)). Journal of magnetic resonance imaging : JMRI. 2012; 36(1):198–205. [PubMed: 22371381]
30. Hambrock T, Somford DM, Huisman HJ, van Oort IM, Witjes JA, Hulsbergen-van de Kaa CA, Scheenen T, Barentsz JO. Relationship between apparent diffusion coefficients at 3.0-T MR imaging and Gleason grade in peripheral zone prostate cancer. Radiology. 2011; 259(2):453–461. [PubMed: 21502392]
31. Somford DM, Hambrock T, Hulsbergen-van de Kaa CA, Futterer JJ, van Oort IM, van Basten JP, Karthaus HF, Witjes JA, Barentsz JO. Initial experience with identifying high-grade prostate cancer using diffusion-weighted MR imaging (DWI) in patients with a Gleason score </= 3 + 3 = 6 upon schematic TRUS-guided biopsy: a radical prostatectomy correlated series. Investigative radiology. 2012; 47(3):153–158. [PubMed: 22293513]
32. Rosenkrantz AB, Sigmund EE, Johnson G, Babb JS, Mussi TC, Melamed J, Taneja SS, Lee VS, Jensen JH. Prostate cancer: feasibility and preliminary experience of a diffusional kurtosis model for detection and assessment of aggressiveness of peripheral zone cancer. Radiology. 2012; 264(1):126–135. [PubMed: 22550312]
33. Bittencourt LK, Barentsz JO, de Miranda LC, Gasparetto EL. Prostate MRI: diffusion-weighted imaging at 1.5T correlates better with prostatectomy Gleason Grades than TRUS-guided biopsies in peripheral zone tumours. European radiology. 2012; 22(2):468–475. [PubMed: 21913058]
34. Kuhl CK, Mielcareck P, Klaschik S, Leutner C, Wardelmann E, Gieseke J, Schild HH. Dynamic breast MR imaging: are signal intensity time course data useful for differential diagnosis of enhancing lesions? Radiology. 1999; 211(1):101–110. [PubMed: 10189459]
35. Tofts PS, Brix G, Buckley DL, Evelhoch JL, Henderson E, Knopp MV, Larsson HB, Lee TY, Mayr NA, Parker GJ, Port RE, Taylor J, Weisskoff RM. Estimating kinetic parameters from dynamic contrast-enhanced T(1)-weighted MRI of a diffusable tracer: standardized quantities and symbols. Journal of magnetic resonance imaging : JMRI. 1999; 10(3):223–232. [PubMed: 10508281]
36. Fennessy FM, Fedorov A, Gupta SN, Schmidt EJ, Tempany CM, Mulkern RV. Practical considerations in T1 mapping of prostate for dynamic contrast enhancement pharmacokinetic analyses. Magnetic resonance imaging. 2012; 30(9):1224–1233. [PubMed: 22898681]
37. Tokuda J, Tuncali K, Iordachita I, Song SE, Fedorov A, Oguro S, Lasso A, Fennessy FM, Tempany CM, Hata N. In-bore setup and software for 3T MRI-guided transperineal prostate biopsy. Physics in medicine and biology. 2012; 57(18):5823–5840. [PubMed: 22951350]
38. Hambrock T, Somford DM, Hoeks C, Bouwense SA, Huisman H, Yakar D, van Oort IM, Witjes JA, Futterer JJ, Barentsz JO. Magnetic resonance imaging guided prostate biopsy in men with repeat negative biopsies and increased prostate specific antigen. The Journal of urology. 2010; 183(2):520–527. [PubMed: 20006859]
39. Hoeks CM, Schouten MG, Bomers JG, Hoogendoorn SP, Hulsbergen-van de Kaa CA, Hambrock T, Vergunst H, Sedelaar JP, Futterer JJ, Barentsz JO. Three-tesla magnetic resonance-guided prostate biopsy in men with increased prostate-specific antigen and repeated, negative, random,

systematic, transrectal ultrasound biopsies: detection of clinically significant prostate cancers. European urology. 2012; 62(5):902–909. [PubMed: 22325447]

40. Overduin CG, Futterer JJ, Barentsz JO. MRI-Guided Biopsy for Prostate Cancer Detection: A Systematic Review of Current Clinical Results. Current urology reports. 2013
41. Aydin H, Kizilgoz V, Tatar IG, Damar C, Ugan AR, Paker I, Hekimoglu B. Detection of prostate cancer with magnetic resonance imaging: optimization of T1-weighted, T2-weighted, dynamic-enhanced T1-weighted, diffusion-weighted imaging apparent diffusion coefficient mapping sequences and MR spectroscopy, correlated with biopsy and histopathological findings. Journal of computer assisted tomography. 2012; 36(1):30–45. [PubMed: 22261768]
42. Kimm SY, Tarin TV, Lee JH, Hu B, Jensen K, Nishimura D, Brooks JD. Methods for registration of magnetic resonance images of ex vivo prostate specimens with histology. Journal of magnetic resonance imaging : JMRI. 2012; 36(1):206–212. [PubMed: 22359365]
43. Mazaheri Y, Bokacheva L, Kroon DJ, Akin O, Hricak H, Chamudot D, Fine S, Koutcher JA. Semiautomatic deformable registration of prostate MR images to pathological slices. Journal of magnetic resonance imaging : JMRI. 2010; 32(5):1149–1157. [PubMed: 21031521]
44. Trivedi H, Turkbey B, Rastinehad AR, Benjamin CJ, Bernardo M, Pohida T, Shah V, Merino MJ, Wood BJ, Linehan WM, Venkatesan AM, Choyke PL, Pinto PA. Use of patient-specific MRI-based prostate mold for validation of multiparametric MRI in localization of prostate cancer. Urology. 2012; 79(1):233–239. [PubMed: 22202553]
45. Vargas HA, Akin O, Franiel T, Mazaheri Y, Zheng J, Moskowitz C, Udo K, Eastham J, Hricak H. Diffusion-weighted endorectal MR imaging at 3 T for prostate cancer: tumor detection and assessment of aggressiveness. Radiology. 2011; 259(3):775–784. [PubMed: 21436085]
46. Hambrock T, Hoeks C, Hulsbergen-van de Kaa C, Scheenen T, Futterer J, Bouwense S, van Oort I, Schroder F, Huisman H, Barentsz J. Prospective assessment of prostate cancer aggressiveness using 3-T diffusion-weighted magnetic resonance imaging-guided biopsies versus a systematic 10-core transrectal ultrasound prostate biopsy cohort. European urology. 2012; 61(1):177–184. [PubMed: 21924545]
47. Ahmed HU, Hindley RG, Dickinson L, Freeman A, Kirkham AP, Sahu M, Scott R, Allen C, Van der Meulen J, Emberton M. Focal therapy for localised unifocal and multifocal prostate cancer: a prospective development study. The lancet oncology. 2012; 13(6):622–632. [PubMed: 22512844]
48. Gangi A, Tsoumakidou G, Abdelli O, Buy X, de Mathelin M, Jacqmin D, Lang H. Percutaneous MR-guided cryoablation of prostate cancer: initial experience. European radiology. 2012; 22(8): 1829–1835. [PubMed: 22752525]
49. Napoli A, Anzidei M, De Nunzio C, Cartocci G, Panebianco V, De Dominicis C, Catalano C, Petrucci F, Leonardo C. Real-time Magnetic Resonance-guided High-intensity Focused Ultrasound Focal Therapy for Localised Prostate Cancer: Preliminary Experience. European urology. 2012
50. D'Amico AV, Cormack RA, Tempany CM. MRI-guided diagnosis and treatment of prostate cancer. The New England journal of medicine. 2001; 344(10):776–777. [PubMed: 11236795]
51. Hata N, Jinzaki M, Kacher D, Cormak R, Gering D, Nabavi A, Silverman SG, D'Amico AV, Kikinis R, Jolesz FA, Tempany CM. MR imaging-guided prostate biopsy with surgical navigation software: device validation and feasibility. Radiology. 2001; 220(1):263–268. [PubMed: 11426008]
52. Cormack RA, D'Amico AV, Hata N, Silverman S, Weinstein M, Tempany CM. Feasibility of transperineal prostate biopsy under interventional magnetic resonance guidance. Urology. 2000; 56(4):663–664. [PubMed: 11018628]
53. D'Amico A V, Tempany CM, Schultz D, Cormack RA, Hurwitz M, Beard C, Albert M, Kooy H, Jolesz F, Richie JP. Comparing PSA outcome after radical prostatectomy or magnetic resonance imaging-guided partial prostatic irradiation in select patients with clinically localized adenocarcinoma of the prostate. Urology. 2003; 62(6):1063–1067. [PubMed: 14665356]
54. Nguyen PL, Chen MH, Zhang Y, Tempany CM, Cormack RA, Beard CJ, Hurwitz MD, Suh WW, D'Amico AV. Updated results of magnetic resonance imaging guided partial prostate brachytherapy for favorable risk prostate cancer: implications for focal therapy. The Journal of urology. 2012; 188(4):1151–1156. [PubMed: 22901567]

55. Fedorov A, Tuncali K, Fennessy FM, Tokuda J, Hata N, Wells WM, Kikinis R, Tempany CM. Image registration for targeted MRI-guided transperineal prostate biopsy. Journal of magnetic resonance imaging : JMRI. 2012; 36(4):987–992. [PubMed: 22645031]
56. Pursley J, Risholm P, Fedorov A, Tuncali K, Fennessy FM, Wells WM, Tempany CM, Cormack RA. A Bayesian nonrigid registration method to enhance intraoperative target definition in image-guided prostate procedures through uncertainty characterization. Medical physics. 2012; 39(11): 6858–6867. [PubMed: 23127078]
57. Fedorov A, Beichel R, Kalpathy-Cramer J, Finet J, Fillion-Robin JC, Pujol S, Bauer C, Jennings D, Fennessy F, Sonka M, Buatti J, Aylward S, Miller JV, Pieper S, Kikinis R. 3D Slicer as an image computing platform for the Quantitative Imaging Network. Magnetic resonance imaging. 2012; 30(9):1323–1341. [PubMed: 22770690]
58. Penzkofer, T.; Tuncali, K.; Fedorov, A.; Tokuda, J.; Song, SE.; Hata, N.; Gupta, GN.; Mulkern, RV.; Fennessy, FM.; Tempany, CM. Multiparametric MRI and pharmakokinetic maps for prostate cancer detection: value in a multireader decision transperineal biopsy study.. Proceedings of the 21st Annual Meeting ISMRM; Salt Lake City, USA. 2013; p. 1770
59. Watanabe H, Igari D, Tanahasi Y, Harada K, Saito M. Development and application of new equipment for transrectal ultrasonography. Journal of clinical ultrasound : JCU. 1974; 2(2):91–98. [PubMed: 4136630]
60. Heijmink SW, Futterer JJ, Strum SS, Oyen WJ, Frauscher F, Witjes JA, Barentsz JO. State-of-the-art uroradiologic imaging in the diagnosis of prostate cancer. Acta Oncol. 2011; 50(Suppl 1):25–38. [PubMed: 21604938]
61. Meirelles LR, Billis A, Cotta AC, Nakamura RT, Caserta NM, Prando A. Prostatic atrophy: evidence for a possible role of local ischemia in its pathogenesis. International urology and nephrology. 2002; 34(3):345–350. [PubMed: 12899225]
62. Lee F, Gray JM, McLeary RD, Lee F Jr. McHugh TA, Solomon MH, Kumasaka GH, Straub WH, Borlaza GS, Murphy GP. Prostatic evaluation by transrectal sonography: criteria for diagnosis of early carcinoma. Radiology. 1986; 158(1):91–95. [PubMed: 3510031]
63. Ellis WJ, Brawer MK. The significance of isoechoic prostatic carcinoma. The Journal of urology. 1994; 152(6 Pt 2):2304–2307. [PubMed: 7526001]
64. Smeenge M, Barentsz J, Cosgrove D, de la Rosette J, de Reijke T, Eggener S, Frauscher F, Kovacs G, Matin SF, Mischi M, Pinto P, Rastinehad A, Rouviere O, Salomon G, Polascik T, Walz J, Wijkstra H, Marberger M. Role of transrectal ultrasonography (TRUS) in focal therapy of prostate cancer: report from a Consensus Panel. BJU international. 2012; 110(7):942–948. [PubMed: 22462566]
65. Beemsterboer PM, Kranse R, de Koning HJ, Habbema JD, Schroder FH. Changing role of 3 screening modalities in the European randomized study of screening for prostate cancer (Rotterdam). International journal of cancer Journal international du cancer. 1999; 84(4):437–441. [PubMed: 10404100]
66. Turkbey B, Pinto PA, Choyke PL. Imaging techniques for prostate cancer: implications for focal therapy. Nature reviews Urology. 2009; 6(4):191–203.
67. Scattoni V, Zlotta A, Montironi R, Schulman C, Rigatti P, Montorsi F. Extended and saturation prostatic biopsy in the diagnosis and characterisation of prostate cancer: a critical analysis of the literature. European urology. 2007; 52(5):1309–1322. [PubMed: 17720304]
68. Ganzer R, Brandtner A, Wieland WF, Fritsche HM. Prospective blinded comparison of real-time sonoelastography targeted versus randomised biopsy of the prostate in the primary and re-biopsy setting. World journal of urology. 2012; 30(2):219–223. [PubMed: 21519851]
69. Salomon G, Kollerman J, Thederan I, Chun FK, Budaus L, Schlomm T, Isbarn H, Heinzer H, Huland H, Graefen M. Evaluation of prostate cancer detection with ultrasound real-time elastography: a comparison with step section pathological analysis after radical prostatectomy. European urology. 2008; 54(6):1354–1362. [PubMed: 18374470]
70. Pallwein L, Mitterberger M, Struve P, Horninger W, Aigner F, Bartsch G, Gradl J, Schurich M, Pedross F, Frauscher F. Comparison of sonoelastography guided biopsy with systematic biopsy: impact on prostate cancer detection. European radiology. 2007; 17(9):2278–2285. [PubMed: 17342485]

71. Brock M, von Bodman C, Palisaar RJ, Loppenberg B, Sommerer F, Deix T, Noldus J, Eggert T. The impact of real-time elastography guiding a systematic prostate biopsy to improve cancer detection rate: a prospective study of 353 patients. The Journal of urology. 2012; 187(6):2039–2043. [PubMed: 22498211]
72. Arani A, Plewes D, Chopra R. Transurethral prostate magnetic resonance elastography: prospective imaging requirements. Magnetic resonance in medicine : official journal of the Society of Magnetic Resonance in Medicine / Society of Magnetic Resonance in Medicine. 2011; 65(2): 340–349. [PubMed: 20882673]
73. Arani A, Plewes D, Krieger A, Chopra R. The feasibility of endorectal MR elastography for prostate cancer localization. Magnetic resonance in medicine : official journal of the Society of Magnetic Resonance in Medicine / Society of Magnetic Resonance in Medicine. 2011; 66(6): 1649–1657. [PubMed: 21574182]
74. Sahebjavaher RS, Baghani A, Honarvar M, Sinkus R, Salcudean SE. Transperineal prostate MR elastography: Initial in vivo results. Magnetic resonance in medicine : official journal of the Society of Magnetic Resonance in Medicine / Society of Magnetic Resonance in Medicine. 2012
75. Chopra R, Arani A, Huang Y, Musquera M, Wachsmuth J, Bronskill M, Plewes D. In vivo MR elastography of the prostate gland using a transurethral actuator. Magnetic resonance in medicine : official journal of the Society of Magnetic Resonance in Medicine / Society of Magnetic Resonance in Medicine. 2009; 62(3):665–671. [PubMed: 19572390]
76. Kemper J, Sinkus R, Lorenzen J, Nolte-Ernsting C, Stork A, Adam G. MR elastography of the prostate: initial in-vivo application. RoFo : Fortschritte auf dem Gebiete der Rontgenstrahlen und der Nuklearmedizin. 2004; 176(8):1094–1099. [PubMed: 15346284]
77. Li S, Chen M, Wang W, Zhao W, Wang J, Zhao X, Zhou C. A feasibility study of MR elastography in the diagnosis of prostate cancer at 3.0T. Acta Radiol. 2011; 52(3):354–358. [PubMed: 21498375]
78. Thormer G, Reiss-Zimmermann M, Otto J, Hoffmann KT, Moche M, Garnov N, Kahn T, Busse H. Novel technique for MR elastography of the prostate using a modified standard endorectal coil as actuator. Journal of magnetic resonance imaging : JMRI. 2012
79. Zhai L, Madden J, Foo WC, Mouraviev V, Polascik TJ, Palmeri ML, Nightingale KR. Characterizing stiffness of human prostates using acoustic radiation force. Ultrasonic imaging. 2010; 32(4):201–213. [PubMed: 21213566]
80. Barr RG, Memo R, Schaub CR. Shear wave ultrasound elastography of the prostate: initial results. Ultrasound quarterly. 2012; 28(1):13–20. [PubMed: 22357224]
81. Brock M, Eggert T, Palisaar RJ, Roghmann F, Braun K, Loppenberg B, Sommerer F, Noldus J, von Bodman C. Multiparametric ultrasound of the prostate: adding contrast enhanced ultrasound to real-time elastography to detect histopathologically confirmed cancer. The Journal of urology. 2013; 189(1):93–98. [PubMed: 23164379]
82. Smeenge M, de la Rosette JJ, Wijkstra H. Current status of transrectal ultrasound techniques in prostate cancer. Current opinion in urology. 2012; 22(4):297–302. [PubMed: 22595778]
83. Zhao HX, Zhu Q, Wang ZC. Detection of prostate cancer with three-dimensional transrectal ultrasound: correlation with biopsy results. The British journal of radiology. 2012; 85(1014):714–719. [PubMed: 21712427]
84. Nelson ED, Slotoroff CB, Gomella LG, Halpern EJ. Targeted biopsy of the prostate: the impact of color Doppler imaging and elastography on prostate cancer detection and Gleason score. Urology. 2007; 70(6):1136–1140. [PubMed: 18158034]
85. Braeckman J, Autier P, Garbar C, Marichal MP, Soviany C, Nir R, Nir D, Michielsen D, Bleiberg H, Egevad L, Emberton M. Computer-aided ultrasonography (HistoScanning): a novel technology for locating and characterizing prostate cancer. BJU international. 2008; 101(3):293–298. [PubMed: 17922870]
86. Braeckman J, Autier P, Soviany C, Nir R, Nir D, Michielsen D, Treurnicht K, Jarmulowicz M, Bleiberg H, Govindaraju S, Emberton M. The accuracy of transrectal ultrasonography supplemented with computer-aided ultrasonography for detecting small prostate cancers. BJU international. 2008; 102(11):1560–1565. [PubMed: 18710457]

87. Simmons LA, Autier P, Zat'ura F, Braeckman J, Peltier A, Romic I, Stenzl A, Treurnicht K, Walker T, Nir D, Moore CM, Emberton M. Detection, localisation and characterisation of prostate cancer by prostate HistoScanning(). BJU international. 2012; 110(1):28–35. [PubMed: 22093966]

88. Salomon G, Spethmann J, Beckmann A, Autier P, Moore C, Durner L, Sandmann M, Haese A, Schlomm T, Michl U, Heinzer H, Graefen M, Steuber T. Accuracy of HistoScanning for the prediction of a negative surgical margin in patients undergoing radical prostatectomy. BJU international. 2013; 111(1):60–66. [PubMed: 22882794]

89. Marks L, Young S, Natarajan S. MRI-ultrasound fusion for guidance of targeted prostate biopsy. Current opinion in urology. 2013; 23(1):43–50. [PubMed: 23138468]

90. Moore CM, Robertson NL, Arsanious N, Middleton T, Villers A, Klotz L, Taneja SS, Emberton M. Image-guided prostate biopsy using magnetic resonance imaging-derived targets: a systematic review. European urology. 2013; 63(1):125–140. [PubMed: 22743165]

91. Singh AK, Kruecker J, Xu S, Glossop N, Guion P, Ullman K, Choyke PL, Wood BJ. Initial clinical experience with real-time transrectal ultrasonography-magnetic resonance imaging fusion-guided prostate biopsy. BJU international. 2008; 101(7):841–845. [PubMed: 18070196]

92. Vourganti S, Rastinehad A, Yerram NK, Nix J, Volkin D, Hoang A, Turkbey B, Gupta GN, Kruecker J, Linehan WM, Choyke PL, Wood BJ, Pinto PA. Multiparametric magnetic resonance imaging and ultrasound fusion biopsy detect prostate cancer in patients with prior negative transrectal ultrasound biopsies. The Journal of urology. 2012; 188(6):2152–2157. [PubMed: 23083875]

93. Miyagawa T, Ishikawa S, Kimura T, Suetomi T, Tsutsumi M, Irie T, Kondoh M, Mitake T. Real-time Virtual Sonography for navigation during targeted prostate biopsy using magnetic resonance imaging data. International journal of urology : official journal of the Japanese Urological Association. 2010; 17(10):855–860. [PubMed: 20807266]

94. Pinto PA, Chung PH, Rastinehad AR, Baccala AA Jr. Kruecker J, Benjamin CJ, Xu S, Yan P, Kadoury S, Chua C, Locklin JK, Turkbey B, Shih JH, Gates SP, Buckner C, Bratslavsky G, Linehan WM, Glossop ND, Choyke PL, Wood BJ. Magnetic resonance imaging/ultrasound fusion guided prostate biopsy improves cancer detection following transrectal ultrasound biopsy and correlates with multiparametric magnetic resonance imaging. The Journal of urology. 2011; 186(4):1281–1285. [PubMed: 21849184]

95. Ukimura O, Desai MM, Palmer S, Valencerina S, Gross M, Abreu AL, Aron M, Gill IS. 3-Dimensional elastic registration system of prostate biopsy location by real-time 3-dimensional transrectal ultrasound guidance with magnetic resonance/transrectal ultrasound image fusion. The Journal of urology. 2012; 187(3):1080–1086. [PubMed: 22266005]

96. Hadaschik BA, Kuru TH, Tulea C, Rieker P, Popeneciu IV, Simpfendorfer T, Huber J, Zogal P, Teber D, Pahernik S, Roethke M, Zamecnik P, Roth W, Sakas G, Schlemmer HP, Hohenfellner M. A novel stereotactic prostate biopsy system integrating pre-interventional magnetic resonance imaging and live ultrasound fusion. The Journal of urology. 2011; 186(6):2214–2220. [PubMed: 22014798]

97. Franiel T, Stephan C, Erbersdobler A, Dietz E, Maxeiner A, Hell N, Huppertz A, Miller K, Strecker R, Hamm B. Areas suspicious for prostate cancer: MR-guided biopsy in patients with at least one transrectal US-guided biopsy with a negative finding--multiparametric MR imaging for detection and biopsy planning. Radiology. 2011; 259(1):162–172. [PubMed: 21233291]

98. Hambrock T, Futterer JJ, Huisman HJ, Hulsbergen-vandeKaa C, van Basten JP, van Oort I, Witjes JA, Barentsz JO. Thirty-two-channel coil 3T magnetic resonance-guided biopsies of prostate tumor suspicious regions identified on multimodality 3T magnetic resonance imaging: technique and feasibility. Investigative radiology. 2008; 43(10):686–694. [PubMed: 18791410]

99. Xu S, Kruecker J, Guion P, Glossop N, Neeman Z, Choyke P, Singh AK, Wood BJ. Closed-loop control in fused MR-TRUS image-guided prostate biopsy. Medical image computing and computer-assisted intervention : MICCAI International Conference on Medical Image Computing and Computer-Assisted Intervention. 2007; 10(Pt 1):128–135. [PubMed: 18051052]

100. Xu S, Kruecker J, Turkbey B, Glossop N, Singh AK, Choyke P, Pinto P, Wood BJ. Real-time MRI TRUS fusion for guidance of targeted prostate biopsies. Computer aided surgery : official journal of the International Society for Computer Aided Surgery. 2008; 13(5):255–264. [PubMed: 18821344]

101. Heijmink SW, Scheenen TW, van Lin EN, Visser AG, Kiemeney LA, Witjes JA, Barentsz JO. Changes in prostate shape and volume and their implications for radiotherapy after introduction of endorectal balloon as determined by MRI at 3T. International journal of radiation oncology, biology, physics. 2009; 73(5):1446–1453.

102. Hu Y, Ahmed HU, Taylor Z, Allen C, Emberton M, Hawkes D, Barratt D. MR to ultrasound registration for image-guided prostate interventions. Medical image analysis. 2012; 16(3):687–703. [PubMed: 21216180]

103. Ives EP, Burke MA, Edmonds PR, Gomella LG, Halpern EJ. Quantitative computed tomography perfusion of prostate cancer: correlation with whole-mount pathology. Clinical prostate cancer. 2005; 4(2):109–112. [PubMed: 16197611]

104. Cyran CC, von Einem JC, Paprottka PM, Schwarz B, Ingrisch M, Dietrich O, Hinkel R, Bruns CJ, Clevert DA, Eschbach R, Reiser MF, Wintersperger BJ, Nikolaou K. Dynamic contrast-enhanced computed tomography imaging biomarkers correlated with immunohistochemistry for monitoring the effects of sorafenib on experimental prostate carcinomas. Investigative radiology. 2012; 47(1):49–57. [PubMed: 21934514]

105. Beer AJ, Eiber M, Souvatzoglou M, Schwaiger M, Krause BJ. Radionuclide and hybrid imaging of recurrent prostate cancer. The lancet oncology. 2011; 12(2):181–191. [PubMed: 20599424]

106. Effert PJ, Bares R, Handt S, Wolff JM, Bull U, Jakse G. Metabolic imaging of untreated prostate cancer by positron emission tomography with 18fluorine-labeled deoxyglucose. The Journal of urology. 1996; 155(3):994–998. [PubMed: 8583625]

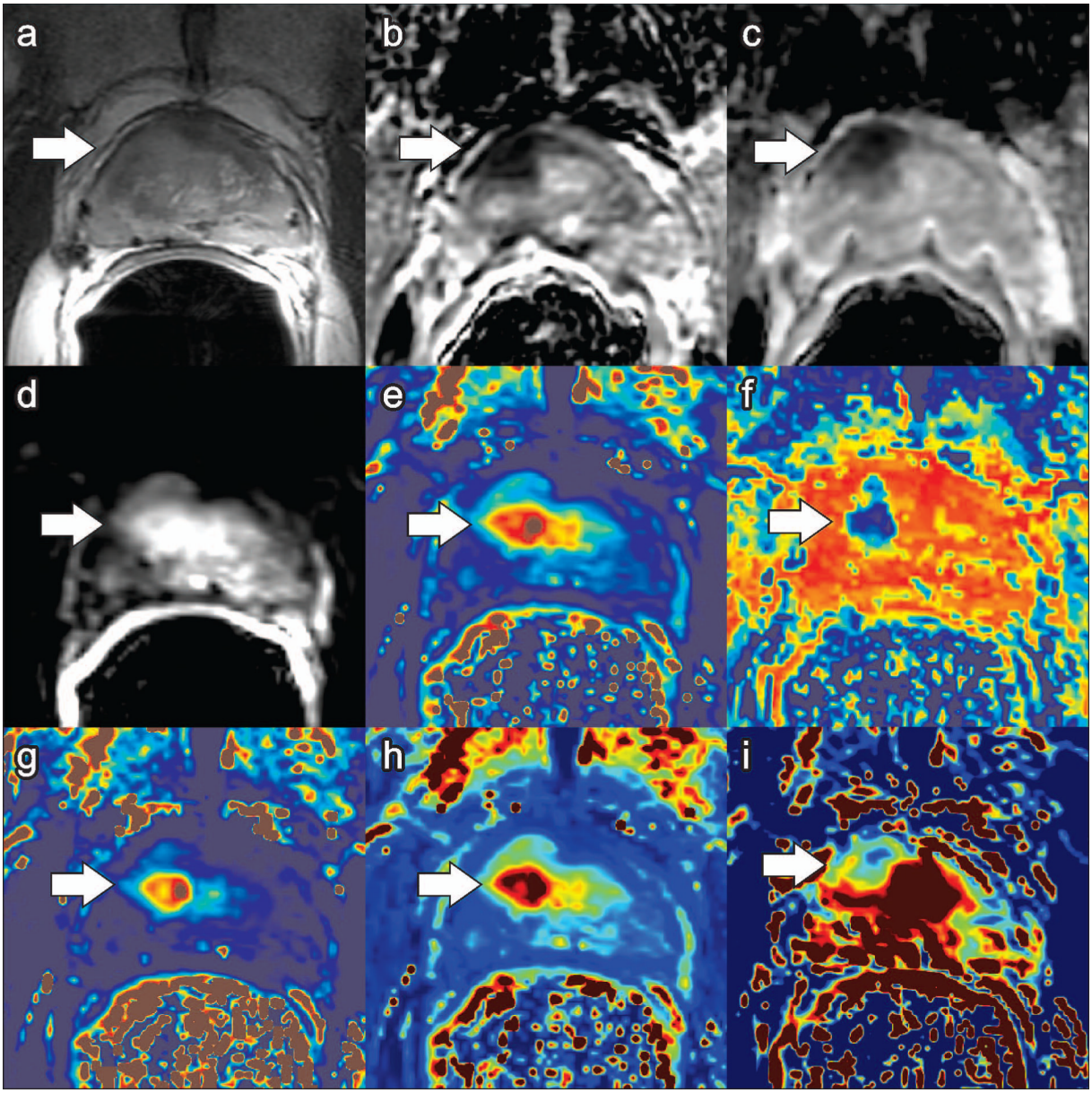


**Figure 1.**
66 year old man, who had prior brachytherapy, with now reelevated PSA. Prostate MRI at 3.0T with endorectal coil (a: T2W, b: ADC500, c: ADC1400, d: Subtraction, e: MaxSlope, f: TTP, g: AUC, h: Ktrans, i: ve) shows abnormal focus of tumor in the right anterior midgland (arrows). The pharmacokinetic analyses show the typical pattern for prostate carcinoma (e-i, color coded from low:blue to high:red, MaxSlope: high, TTP: low, AUC: high, Ktrans: high and ve: low, pharmacokinetic analyses performed using Oncoquant, GE Healthcare).

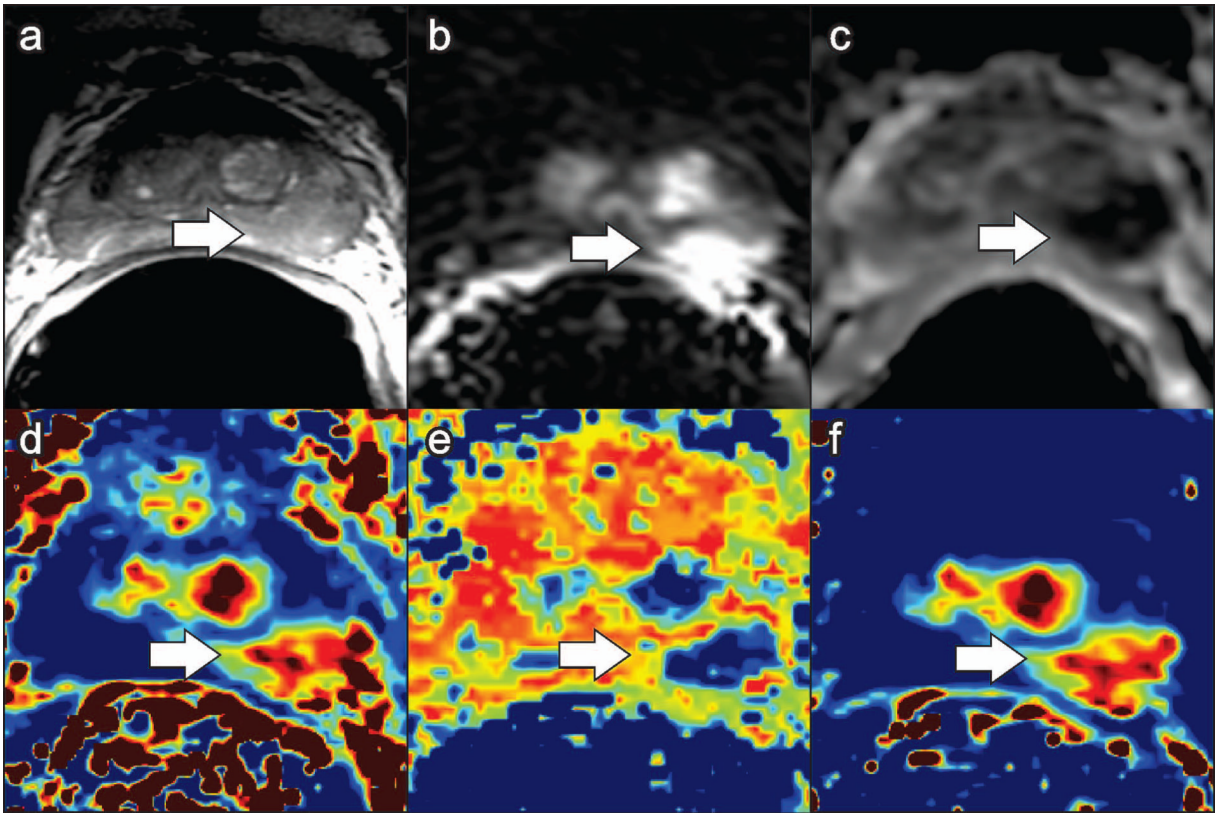


**Figure 2.**

65 year old man with elevated PSA. The multiparametric MRI (a: T2W, b: DCE subtraction, c: ADC500, d: MaxSlope, e: TTP, f: AUC) shows a suspicious lesion in the left peripheral zone (arrows) with a suspicious contrast enhancement pattern (b) and restricted diffusion (c). Pharmacokinetic analyses (d-e, color coded from low:blue to high:red) show a high value for maximum slope (d) and area under the curve (e), and a short value for time-to-peak in the suspicious area. Histologic examination after prostate biopsy resulted in a Gleason 3+4=7 prostate cancer in the left peripheral zone.

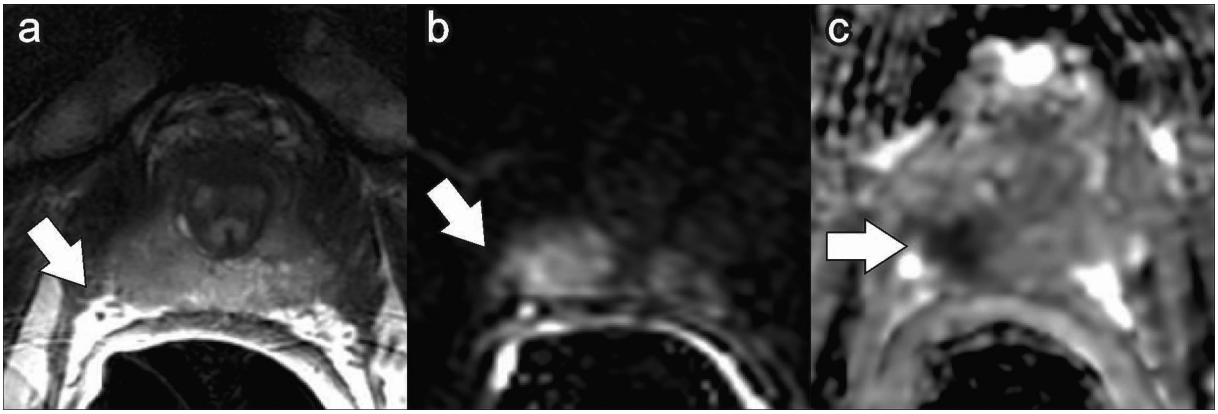


**Figure 3.**
63 year old man with biopsy proven prostate cancer. The multiparametric MRI (a: axial T2W, b: DCE subtraction, c: ADC1400) shows extracapsular extension into the right neurovascular bundle (arrow) as indicated by focal capsular bulging (a), contrast uptake (b) and restricted diffusion (c).

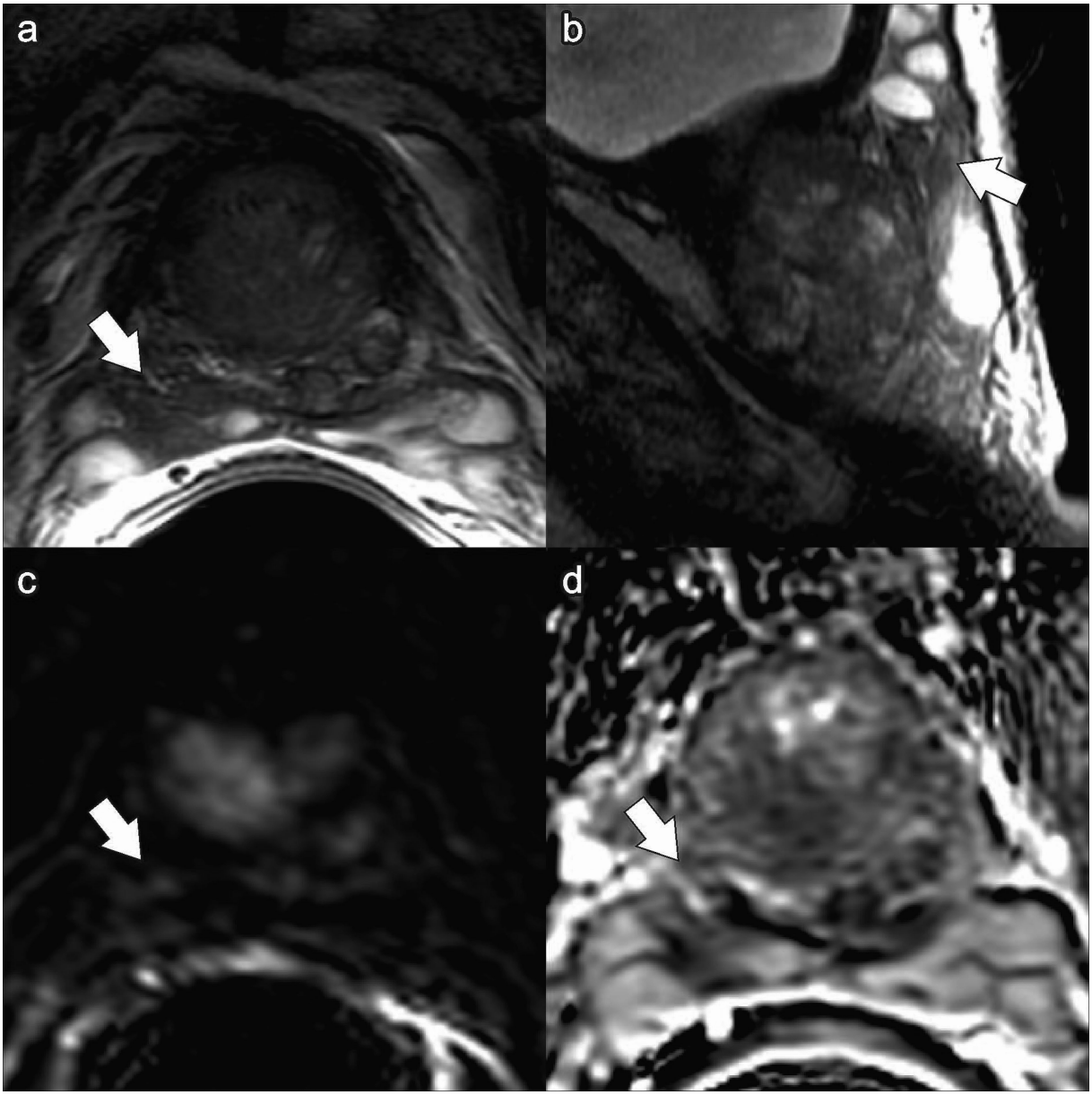


**Figure 4.**
Multiparametric prostate MRI (a: axial T2W, b: sagittal T2W, c: DCE subtraction, d: ADC map (b=500)) of a 60 year old patient with biopsy-proven prostate cancer (Gleason 4+3=7) and rapidly rising PSA. The MRI shows signal abnormalities in the medial part of the seminal vesicle suggestive for seminal vesicle invasion (arrows).

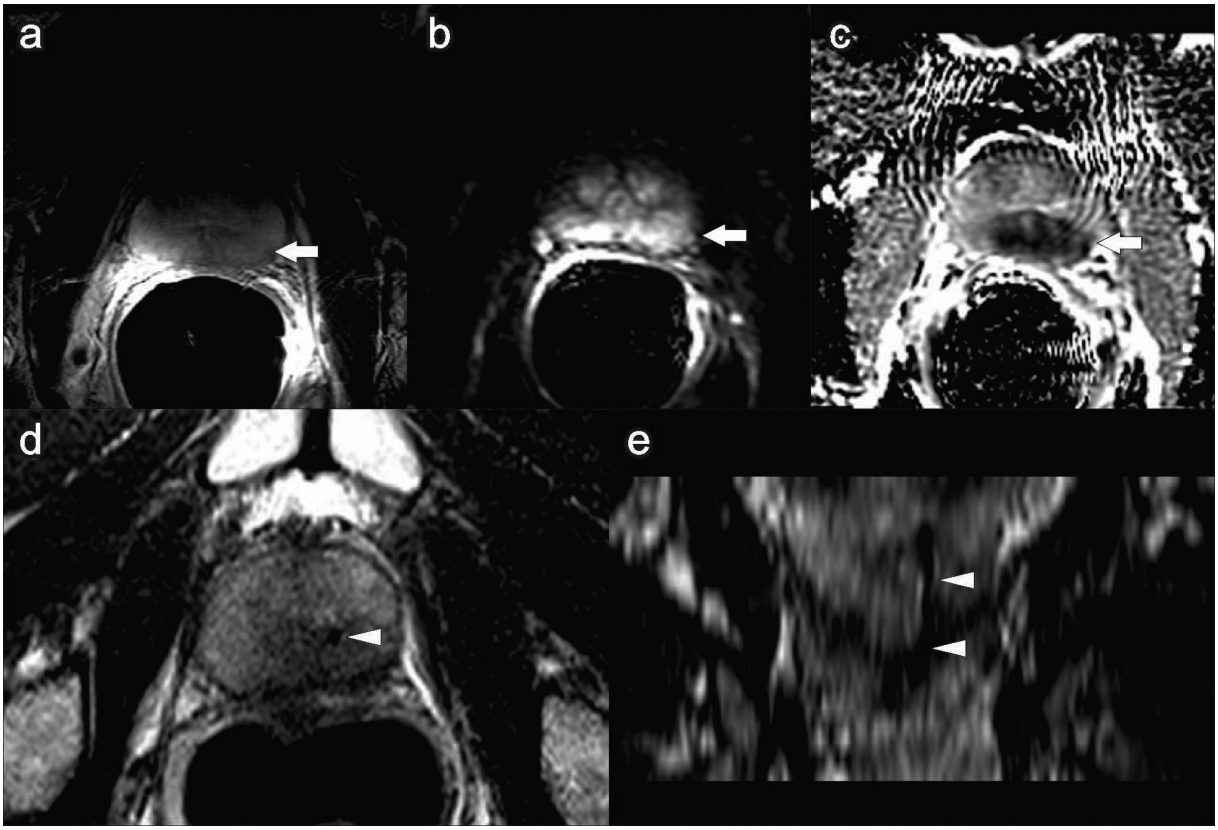


**Figure 5.**
61 year old patient after external beam radiation and hormonal therapy with recent PSA re-elevation. Multiparametric MRI (a: T2W, b: DCE subtraction, c: ADCb1400) shows a suspicious lesion in left peripheral zone (arrows). A MRI guided prostate biopsy (d: axial T2W, e: 3D Slicer coronal reformat) was performed targeting the suspicious area (arrows: needle position in left peripheral zone).

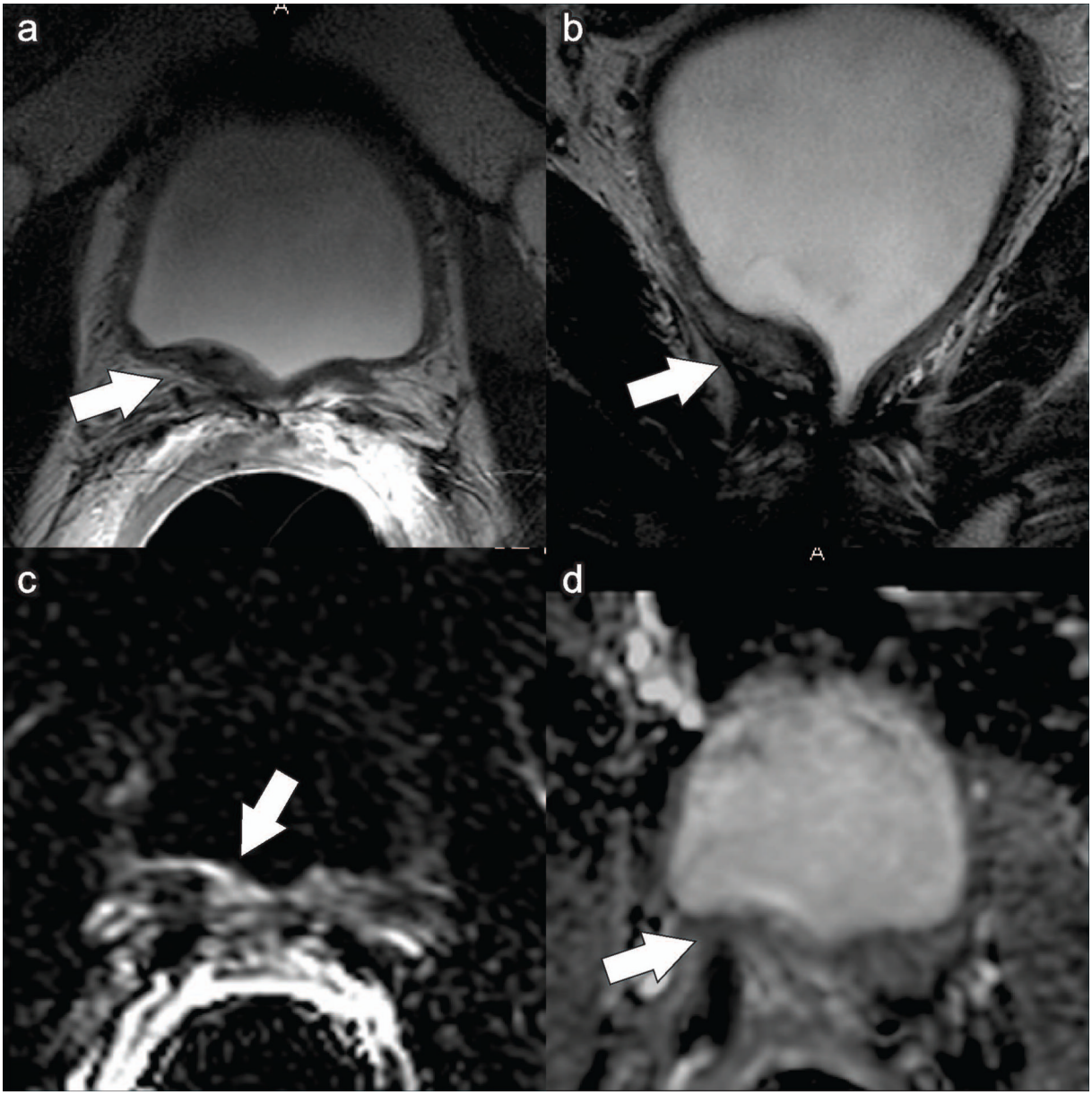


**Figure 6.**
54 year old man with Gleason 4+4=8 prostate cancer, who underwent prostatectomy 6 years ago, now presenting with reelevated PSA. The multiparametric MRI (a: axial T2W, b: coronal T2W, c: DCE subtraction, d: ADCb1400) reveals a right side lesion with focal soft tissue enlargement (a+b), contrast enhancement (c), and diffusion restriction (d) in the surgical bed, suggestive of local recurrence (arrows).

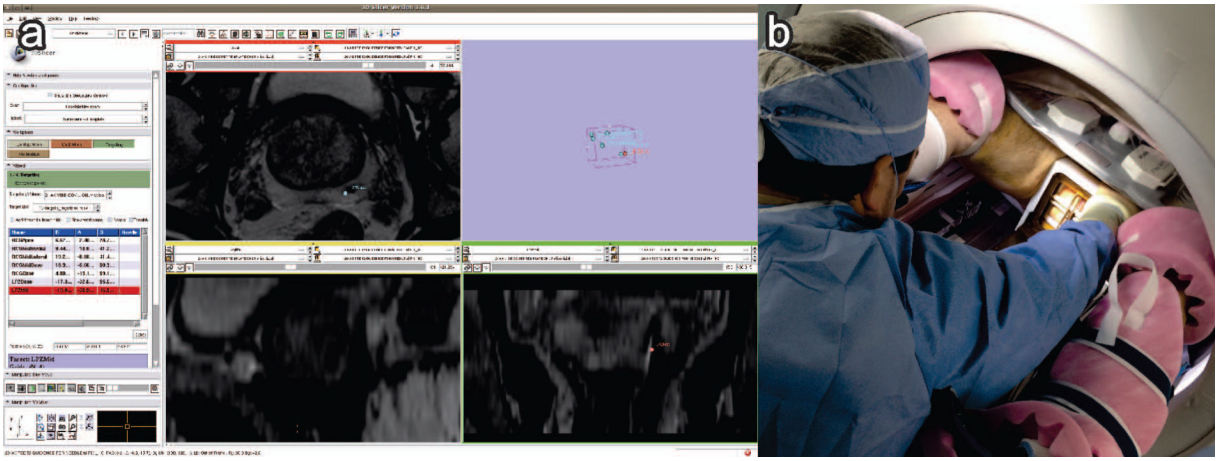


**Figure 7.**
MRI guided, transperineal prostate biopsy (Siemens Verio 3.0T, Open Bore [70cm], Siemens Healthcare, Erlangen, Germany): (a) biopsy plan derived from preprocedural multiparametric MRI in a multi-reader setting visualized in 3D Slicer (www.slicer.org), a target is seen on the right peripheral zone and (b) sampled in an in-bore setting using a template based approach.

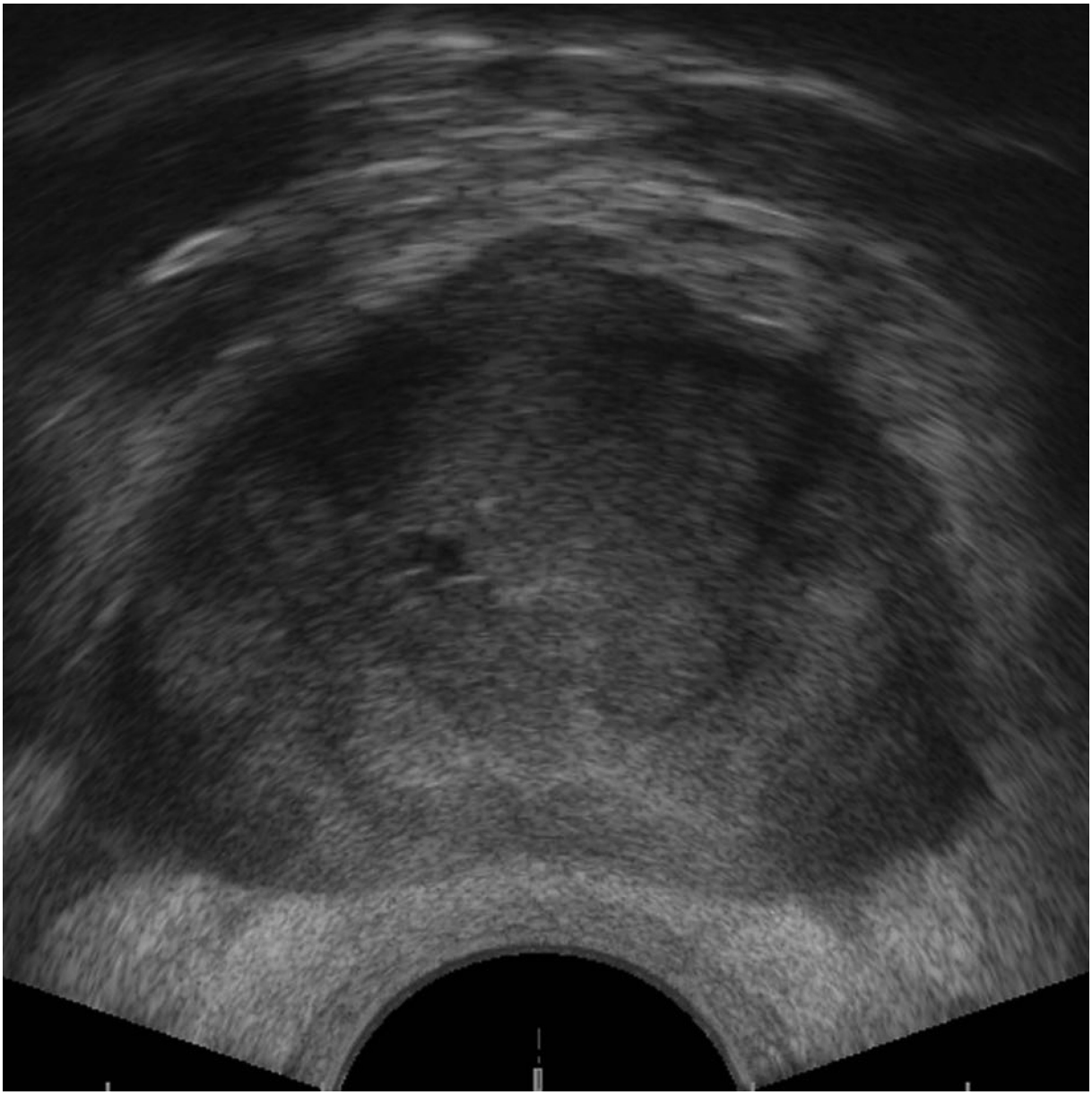

**Figure 8.**
TRUS ultrasound in a 71 year old with bilateral prostate cancer. While the prostate borders are clearly visible and some intraprostatic structure is seen, no suspicious lesions were identified.

**Table 1**

Example Prostate MRI protocol at 3.0 Tesla (FSE: fast spin echo, SPGR: spoiled gradient echo, EPI: single shot echo planar imaging, DCE: dynamic contrast enhanced, DWI: diffusion weighted imaging, TR: repetition time, TE: echo time, FoV: field of view, Gd: Gadolinium-enhanced)

| | T2W (3-plane) | Axial T1W | Axial DWI | Axial 3D DCE | Axial T1 post-Gd | Axial T1 (large FoV) |
|---|---|---|---|---|---|---|
| Sequence | FSE | SPGR | EPI | SPGR | SPGR | SPGR |
| TR | 3500 | 385 | 2500 | 3.6 | 385 | 225 |
| TE | 102 | 6.2 | 65.7 | 1.3 | 6.2 | 3.3 |
| Flip Angle | 90 | 65 | | 15 | 65 | 75 |
| FoV | 16 | 16 | 18*10.8 | 26 | 16 | 35-40 |
| Slice Thickness | 3 | 3 | 3 | 5 | 3 | 5 |
| Spacing | 0 | 0 | 0 | 0 | 0 | 1 |
| Matrix | 384×224 | 384×192 | 128×96 | 256×160×20 | 384×192 | 256×160 |
| Remarks | | | b-values: 0, 500, 1400 sec/ $mm^2$ | | | |